

## Structure of Monatomic Steps on the Si(001) Surface

P. Bogusławski,\* Q.-M. Zhang, Z. Zhang, and J. Bernholc  
North Carolina State University, Raleigh, North Carolina 27695-8202  
(Received 10 January 1994)

The atomic and electronic structure of the stepped Si(001) surface is investigated by *ab initio* molecular dynamics. All configurations considered by us are unstable with respect to the buckling of the surface dimers. The ground state reconstruction depends on the type of the step and, in some cases, is different from that of the flat surface. The observed differences between the filled-state and the empty-state scanning tunneling microscopy images are due to differences in wave function shapes rather than tip-induced reconstruction.

PACS numbers: 68.35.Bs, 61.16.Ch, 73.20.At

Steps are an important component of the real Si(001) surface. Their presence may result from the intrinsic instability of the infinite flat Si(001) surface [1], or may trivially be due to the fact that a micron-size area will not be smooth on an atomic scale. Steps can also be intentionally created by choosing a finite miscut angle for vicinal surfaces. Much effort was recently devoted to mapping out the phase diagram of the Si(001) surface, which turned out to be surprisingly rich [2–6]. Even in the case of zero temperature and no external strain, the global ground state configuration of the Si(001) surface, i.e., the density, the height, and the shape of steps vary as a function of the miscut angle. The steps are double-layer high for miscut angles exceeding about  $6^\circ$ , and monolayer high for angles less than about  $1.5^\circ$ . (For intermediate values, complex sequences of single- and double-layer steps occur [6].) Furthermore, for a very low miscut, steps form sinusoidal patterns [7]. The driving force behind this large-scale surface reorganization is the anisotropic surface strain. The complexity of the phase diagram stems from an attempt by the surface to minimize its strain energy through the formation of domains with optimal shapes at the expense of introducing steps. The domains extend from one step edge to the other, and thus their lateral size typically ranges from tens to thousands of angstroms. Vertically, strain domains extend to about 100 monolayers below the free surface [8]. Such a large size of the domains makes the usage of heuristic approaches (model interatomic potentials, or continuum medium theory) both appropriate methodologically and necessary from the computational viewpoint.

Less is known about the *local* structure of Si(001). There has been considerable controversy concerning the question of whether the dimers are symmetric or buckled [9,10]. The most recent experimental results [11–13] demonstrate convincingly that the dimers are buckled (i.e., the two atoms forming a dimer have different  $z$  coordinates), and that the low-temperature ground state consists of coexisting regions of  $p(2\times 2)$  and  $c(2\times 4)$  reconstructions [11]. The most recent *ab initio* calculations [10,14,15] confirm the picture of asymmetric dimers, originally proposed by Chadi [16]. These calculations were performed for the ideal flat surface only. They show that the buckling involves charge transfer between

two atoms forming a dimer, which gives the energy gain of about 0.1 meV per dimer and opens a Peierls gap [15]. Since charge transfer effects are not taken into account by model interatomic potentials, they predict symmetric dimers and a metallic surface.

In this Letter, we investigate, for the first time, the energetics and atomic and electronic structure of monatomic height steps at the Si(001) surface by an *ab initio* technique. In all cases studied by us, the symmetric dimer structures at step edges are unstable with respect to buckling, and the resulting reconstruction leads to an insulating structure. In some cases, however, the ground state reconstruction is different from that of a flat surface. Finally, an analysis of our simulated scanning tunneling microscope (STM) images provides a comprehensive interpretation of the experimental data.

The calculations were carried out within the *ab initio* molecular dynamics scheme [17] and the local density approximation (LDA). We used pseudopotentials with  $s$  and  $p$  nonlocalities, a seven-layer-Si slab with seven layers of vacuum, and a kinetic energy cutoff of 8 Ry for the plane waves. The dangling bonds at the bottom surface of the slab were saturated with H atoms and the two bottom layers of Si atoms were kept fixed at the ideal bulk sites. The in-plane unit cell period was  $6\times 4$ , resulting in up to 168 Si and 48 H atoms in the unit cell. Because of the large size of the cell, summations over the Brillouin zone were approximated by the  $\Gamma$  point. As shown by Dabrowski and Scheffler [10], these choices give the buckling energy with a precision of about 0.03 eV per surface dimer (half of which is due to the single  $\mathbf{k}$  point sampling), which is certainly sufficient to compare the relative energetics of the various reconstructions of the step edge. However, the computation of the step formation energy by an *ab initio* technique is not technically possible at present, since it would require a series of calculations for supercells containing over 1000 atoms [8]. To speed up the search for minimum energy configurations, the atoms were relaxed according to an efficient scheme which uses Newtonian dynamics with a special friction force for the atoms [18], while the electrons follow the motion of the atoms according to the Car-Parrinello equations [17]. The codes were highly parallel and run on 4 processors of a Cray C90 supercomputer

with the speed of 2.3 Gflops.

Before discussing the stepped surface, an analysis of the flat surface is important. We considered reconstructions with  $s(2\times 1)$  symmetric dimers,  $b(2\times 1)$  buckled dimers, and alternating buckled dimers in  $p(2\times 2)$  and  $c(2\times 4)$  structures. In agreement with previous calculations [10,14,15], we find that symmetric dimers represent an unstable configuration of the Si(001) surface. Compared to  $s(2\times 1)$ , a  $b(2\times 1)$  reconstruction with a buckling of 0.51 Å lowers the total energy by 0.10 eV per surface dimer. The computed ground state of the flat Si(001) surface is the  $c(2\times 4)$  reconstruction, which induces an energy gain of 0.24 eV per surface dimer, and a buckling of 0.72 Å. The  $p(2\times 2)$  reconstruction is nearly degenerate energetically with the  $c(2\times 4)$ , since its energy is higher by only 8 meV per surface dimer. In this case the buckling is 0.71 Å.

We will now consider the stepped Si(001) surface. Here, we focus on surfaces with miscut angle less than about 1.5°, in which case all steps are of monolayer height. There are two types of such steps, denoted by  $S_A$  and  $S_B$  after Chadi [19]. In the case of  $S_A$ , the dimers on the upper terrace are perpendicular to the step edge, and for  $S_B$  they are parallel to the edge. Further, the  $S_B$  step may be terminated either by a rebonded or a nonrebonded edge. Thus, for symmetric dimers, there are three nonequivalent configurations. The buckling of dimers substantially increases the number of possible stepped configurations. First, the reconstructions at the upper and the lower terrace may be different. Consequently, considering only two reconstructions of the terraces,  $p(2\times 2)$  and  $c(2\times 4)$ , one obtains 12 possible configurations. Second, various possible reconstructions of the step edges further increase the number of possible configurations. For example, there are two possible variants of the  $S_A$  edge (see below). Because of the computational constraints we could not investigate all possibilities and studied only eight paradigmatic cases.

Before discussing the results in detail, we show in Fig. 1 the calculated equilibrium configurations of the step edges. In general, it is apparent from Figs. 1(a) and 1(c) that the magnitude of the buckling is comparable to interlayer spacing. Step  $S_A$  shown in Fig. 1(a) is in a  $S_{A1}$  configuration (discussed below in more detail), with the  $c(2\times 4)$  reconstruction on both the higher and the lower terrace. In this case we do not discuss the configuration with symmetric dimers, which is unstable. The edge of  $S_{A1}$  is not strongly reconstructed, i.e., its structure on both terraces is close to that of the flat surface. Figures 1(b) and 1(c) show the nonrebonded  $S_B$  edge. To highlight the magnitude of the dimer asymmetry we compare two cases: the first one [Fig. 1(b)] is that of symmetric dimers, which is a metastable saddle-point configuration; in the second one [Fig. 1(c)] the dimers are buckled in a  $p(2\times 2)$  pattern, which is the lowest energy configuration for  $S_B$ . The dimers on both terraces and the step edge reconstruct very strongly, but the bond

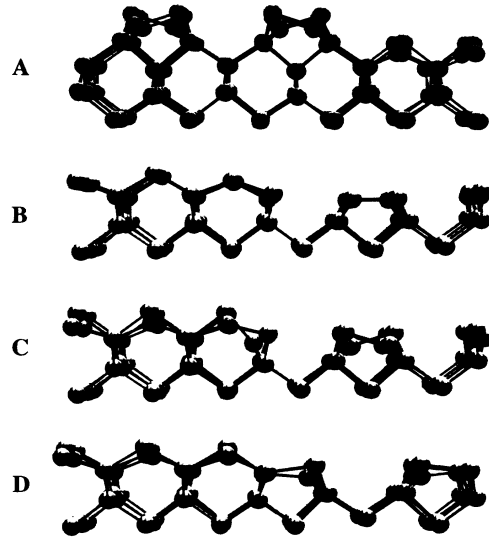


FIG. 1. Calculated equilibrium configurations of (a) step  $S_{A1}$ ; (b) step  $S_B$  with a nonrebonded edge and symmetric dimers; (c) step  $S_B$  with a nonrebonded edge and a  $p(2\times 2)$  reconstruction; and (d) step  $S_B$  with a rebonded edge and a  $p(2\times 2)$  reconstruction. See text.

lengths are approximately preserved. The atoms at the edge move the most, due to their lower coordination. This reconstruction is of electronic origin, since it is driven by buckling of the dimers from the upper terrace. Similar features also characterize the rebonded  $S_B$  edge [Fig. 1(d)].

In the case of step  $S_A$ , the alternating buckling of the dimers at the first row of the upper terrace is induced by the geometry of the step edge [20]. There are two possible variants. The first one, called here  $S_{A1}$ , is observed experimentally [21,22]. In this variant, the “up” atoms at the edge of the upper plane are aligned with the center of the dimer in the lower plane, while the “down” atoms are aligned with the gap between the dimer rows in the lower plane. In the second variant, denoted here by  $S_{A2}$ , the tilt of the dimers on the upper plane has the opposite sign. For both  $S_{A1}$  and  $S_{A2}$ , the reconstruction of the upper plane has  $c(2\times 4)$  periodicity. We considered two reconstruction patterns of the lower terrace,  $c(2\times 4)$  and  $p(2\times 2)$ . For  $S_{A1}$ , the buckling on the upper terrace is 0.71 Å, which is very close to the value calculated for the flat surface. For the lower terrace, the  $c(2\times 4)$  and the  $p(2\times 2)$  reconstructions are energetically degenerate (within the accuracy of the calculations). However, the buckling energy is 0.14 eV per surface dimer, which is less than that of the flat surface (0.24 eV). The buckling at the lower plane, about 0.62 Å for both reconstructions, is also smaller than for the flat surface. The second step geometry,  $S_{A2}$  has its total energy equal to that of  $S_{A1}$  within the accuracy of the calculations. This is unexpected, since this configuration was not observed experimentally.

Step  $S_B$  can exist in two variants, rebonded and nonre-

bonded, and both variants have been observed in STM experiments [22]. However, the nonrebonded step is often observed with additional dimers on the adjacent dimer row [23]. We considered the rebonded step and the nonrebonded step without the additional dimers, with both  $c(2\times 4)$  and  $p(2\times 2)$  reconstructions. Our findings can be summarized as follows: (i) For the *rebonded* edge, the  $p(2\times 2)$  reconstruction is more stable than the  $c(2\times 4)$  by 80 meV per surface dimer. This may explain why in the high-resolution image [24] the  $p(2\times 2)$  periodicity is seen. The energy lowering in the  $p(2\times 2)$  case is induced by a pronounced reconstruction of the step edge, which is buckled by 0.58 Å. The buckling of the terraces is about 2 times smaller than that of the flat surface. (ii) In the case of the *nonrebonded* edge with  $p(2\times 2)$  periodicity, the buckling is 0.74 Å at the edge, which is more than that for the flat surface, and 0.6 Å for the middle row. The row of dimers at the lower terrace is buckled by 0.69 Å. (iii) The energy difference between the rebonded and nonrebonded edges strongly depends on the surface reconstruction. For the  $b(2\times 1)$  reconstruction on both terraces the energy of the rebonded edge is lower by 0.8 eV per edge atom, which reduces to 0.3 eV per edge atom for  $c(2\times 4)$ . The observation of both rebonded and nonrebonded configurations indicates that the barrier for the transformation to the rebonded edge is substantial [25]. Interestingly, the energy difference of 0.3 eV between the fully reconstructed rebonded and nonrebonded edges is close to 0.33 eV per edge atom obtained for the symmetric dimers with the Tersoff potential [26].

The Si(001) stepped surface has been the subject of many beautiful STM studies [2,4,11,21,22,24]. In the last part of this Letter we will support our results by simulating STM images and comparing them with the experimental data. The images were computed as a function of the bias voltage and the current intensity. For the case of negative sample voltage, the current tunnels from the sample to the tip, and thus the corresponding image probes the filled states. For the positive voltage case, the image probes the empty surface states. According to Tersoff and Hamann [27], the contribution of a given state to the tunneling current is proportional to the square of its wave function. The total current is approximated by a sum of such contributions in the appropriate energy interval. The isosurfaces of the tunneling current

plotted in Fig. 2 were obtained using an energy interval of 0.3 eV centered at  $-0.5$  eV below the top of the valence band for the filled state image, and at  $+0.8$  eV for the empty state image. This analysis was performed for most of the studied geometries. In all cases, the same qualitative differences between the filled and empty state images were found. As an example, we discuss in detail the results obtained for the  $S_B$  nonrebonded step with the  $p(2\times 2)$  reconstruction.

Figure 2(a) shows the filled state image. Note the formation of a weak bond between atoms at the step edge and atoms from the first row of the lower terrace. The bonding occurs in spite of the nonrebonded character of the edge, and is due to the close proximity of the two atoms induced by the edge reconstruction. The positions of the maxima of the isosurface along the  $z$  axis correspond with the positions of the "up" atoms, while the "down" atoms are nearly not seen. The apparent buckling is about 1.2 Å, which is much more than the actual value of 0.7 Å. In contrast, on the empty state image shown in Fig. 2(b), the dimers appear to be nearly symmetric. A small apparent buckling is visible, but its sign has changed: the up atoms appear to be lower than the down atoms by about 0.1 Å.

The above results can be understood by analyzing the wave functions contributing to the STM images. For flat surfaces with  $2\times 1$  periodicity, surface states form two bands with energies in the vicinity of the band gap [16,28]. The lower, occupied band is resonant with the top of the bulk valence band. Its wave function at  $\Gamma$  is built up mainly from the  $p_z$  orbitals of the up atoms. The upper band, which is in the upper part of the gap, is empty, and its wave function consists of the dangling bonds of the down atoms [29]. This buckling-induced charge transfer is universal for both flat and stepped surfaces. Consequently, the filled state image, which reflects the occupied states of the up atoms, has the tendency to overestimate the apparent buckling. In the empty state image, tunneling occurs to the dangling bonds of the down atoms, which makes the dimers appear symmetric.

The second difference between the filled and empty state images are the positions of the apparent maxima and minima. In the case of filled state images, the maxima are on top of up atoms and/or between them. This results in the zigzag-shaped pattern observed for both

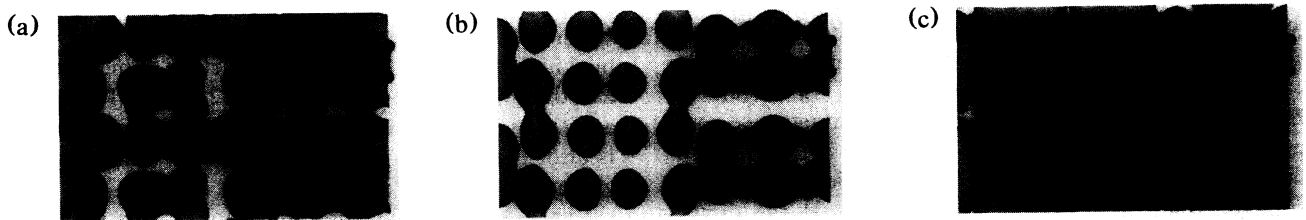


FIG. 2. Simulated STM images of step  $S_B$  with a nonrebonded edge. (a) The filled-state image at a "high-current" condition; (b) the empty-state image at a "high-current" condition; and (c) the filled-state image at a "low-current" condition. The positions of the topmost atoms are denoted by filled circles. See text.

$p(2\times 2)$  and  $c(2\times 4)$  reconstructions. The apparent minima are situated between the neighboring rows of dimers. This situation is reversed for the empty states. In this case, the apparent minimum is positioned in the middle of the dimers. This is clearly seen in, e.g., Fig. 4 of Ref. [24], and is also reproduced by our simulated images [see the dimer row on the lower terrace in Fig. 2(b)]. The occurrence of the minimum is due to the fact that the empty states are conduction band states with antibonding character, which leads to wave functions having a node between the two dimer atoms.

In order to investigate the influence of the second parameter, the current intensity, we compare isosurfaces with high [Fig. 2(a)] and low [Fig. 2(c)] values. It is clear from Figs. 2(a) and 2(c) that the decrease of the current does not introduce any qualitatively new features, but only causes an overall smoothing of the image. In particular, the apparent buckling becomes less pronounced.

The difference between the filled and the empty state images has been observed and discussed by Kochanski and Griffith [24]. Their interpretation of this effect assumes that the electric field between the tip and the sample is strong enough to drive a transition from buckled to symmetric dimers. Our results provide an alternative and more satisfactory interpretation of experiment, based on the calculated electronic structure of the filled and empty states only, and not requiring any changes in the positions of the surface atoms.

In summary, we studied the stepped Si(001) surface by *ab initio* molecular dynamics. We considered monolayer high  $S_A$  and  $S_B$  steps, and  $s(2\times 1)$ ,  $b(2\times 1)$ ,  $p(2\times 2)$ , and  $c(2\times 4)$  reconstructions. Concerning the atomic structure, we find that symmetric dimers are unstable with respect to buckling for all configurations considered here. The buckling amounts to about 0.7 Å, i.e., is comparable to the interlayer spacing, and leads to an energy gain of about 0.2 eV/dimer. In general, the  $c(2\times 4)$  and  $p(2\times 2)$  structures are energetically close. The exceptions are the  $S_A$  step, where the  $c(2\times 4)$  reconstruction is induced by the edge geometry, and the  $S_B$  nonrebonded step, for which the  $p(2\times 2)$  structure is more stable than the  $c(2\times 4)$  structure by 80 meV per dimer. All studied stepped systems are insulating, and there are no edge-induced states in the gap. Finally, we simulated STM images and compared them with experiment. The observed qualitative differences between the filled- and empty-state images are explained by shapes of the surface state wave functions, without assuming tip-induced reconstructions.

We would like to thank Professor C. Roland for valuable discussions. We would also like to thank V. Shaffer for his expert help in parallelizing our codes. This work was supported by NSF, Grant No. DMR-9100063, and ONR, Grant No. N00014-91-J-1516. The calculations were carried out at the Pittsburgh Supercomputing Center.

\*Permanent address: Institute of Physics, Polish Academy of Sciences, 02-668 Warsaw, Poland.

- [1] O. L. Alerhand, D. Vanderbilt, R. D. Maede, and J. Joannopoulos, Phys. Rev. Lett. **61**, 1973 (1988).
- [2] O. L. Alerhand, A. N. Berker, J. Joannopoulos, D. Vanderbilt, R. J. Hamers, and J. E. Demuth, Phys. Rev. Lett. **64**, 2406 (1990).
- [3] B. S. Swartzentruber, Y.-W. Mo, R. Kariotis, M. G. Lagally, and M. B. Webb, Phys. Rev. Lett. **65**, 1913 (1990).
- [4] J. J. de Miguel, C. E. Aumann, R. Kariotis, and M. G. Lagally, Phys. Rev. Lett. **67**, 2830 (1991).
- [5] X. Tong and P. A. Bennett, Phys. Rev. Lett. **67**, 101 (1991).
- [6] E. Pehlke and J. Tersoff, Phys. Rev. Lett. **67**, 465 (1991); **67**, 1290 (1991).
- [7] R. M. Tromp and M. C. Reuter, Phys. Rev. Lett. **68**, 820 (1992); J. Tersoff and E. Pehlke, *ibid.* **68**, 816 (1992).
- [8] T. W. Poon, S. Yip, P. S. Ho, and F. F. Abraham, Phys. Rev. Lett. **65**, 2161 (1990).
- [9] See, e.g., J. E. Rowe and G. K. Wertheim, Phys. Rev. Lett. **69**, 550 (1992); F. J. Himpsel, *ibid.* **69**, 551 (1992); D. S. Lin, J. A. Carlisle, T. Miller, and T.-C. Chiang, **69**, 552 (1992), and the references therein.
- [10] J. Dabrowski and M. Scheffler, Appl. Surf. Sci. **56-58**, 15 (1992).
- [11] R. A. Wolkow, Phys. Rev. Lett. **68**, 2636 (1992).
- [12] E. Landemark, C. J. Karlsson, Y. C. Chao, and R. I. G. Uhrberg, Phys. Rev. Lett. **69**, 1588 (1992).
- [13] E. Fontes, J. R. Patel, and F. Comin, Phys. Rev. Lett. **70**, 2790 (1993).
- [14] N. Roberts and R. J. Needs, Surf. Sci. **236**, 112 (1990).
- [15] J. E. Northrup, Phys. Rev. B **47**, 10032 (1993).
- [16] J. D. Chadi, Phys. Rev. Lett. **43**, 43 (1979).
- [17] R. Car and M. Parrinello, Phys. Rev. Lett. **55**, 2471 (1985).
- [18] C. Wang, Q.-M. Zhang, and J. Bernholc, Phys. Rev. Lett. **69**, 3789 (1992).
- [19] J. D. Chadi, Phys. Rev. Lett. **59**, 1691 (1987).
- [20] A strong buckling induced by geometry rather than electronic processes was also observed for solitary dimer rows on Si(001) by Bedrossian and Kaxiras [21]. In their case the effect is more pronounced than for the  $S_A$  edge.
- [21] P. Bedrossian and E. Kaxiras, Phys. Rev. Lett. **70**, 2589 (1993).
- [22] R. J. Hammers, R. M. Tromp, and J. E. Demuth, Phys. Rev. B **34**, 5343 (1986).
- [23] R. J. Hammers, U. K. Kohler, and J. E. Demuth, J. Vac. Sci. Technol. A **8**, 195 (1990).
- [24] G. P. Kochanski and J. E. Griffith, Surf. Sci. **249**, L293 (1991).
- [25] Surfaces used for STM experiments are typically annealed at high temperatures (at which nonrebonded edges may form) and then quenched to room temperature.
- [26] J. Tersoff, Phys. Rev. B **39**, 5566 (1989).
- [27] J. Tersoff and D. R. Hamann, Phys. Rev. Lett. **50**, 1998 (1983).
- [28] J. Pollmann, P. Kruger, and A. Mazur, J. Vac. Sci. Technol. B **5**, 945 (1987).
- [29] For  $p(2\times 2)$  and  $c(2\times 4)$  surfaces, both bands are further split into doublets due to the doubling of the in-plane period [15].

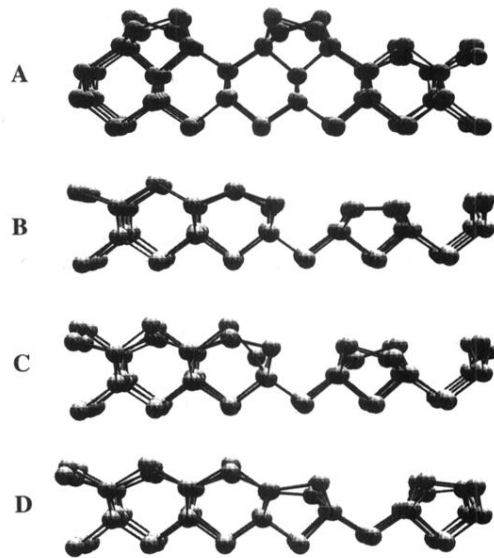


FIG. 1. Calculated equilibrium configurations of (a) step  $S_{A1}$ ; (b) step  $S_B$  with a nonrebonded edge and symmetric dimers; (c) step  $S_B$  with a nonrebonded edge and a  $p(2 \times 2)$  reconstruction; and (d) step  $S_B$  with a rebonded edge and a  $p(2 \times 2)$  reconstruction. See text.

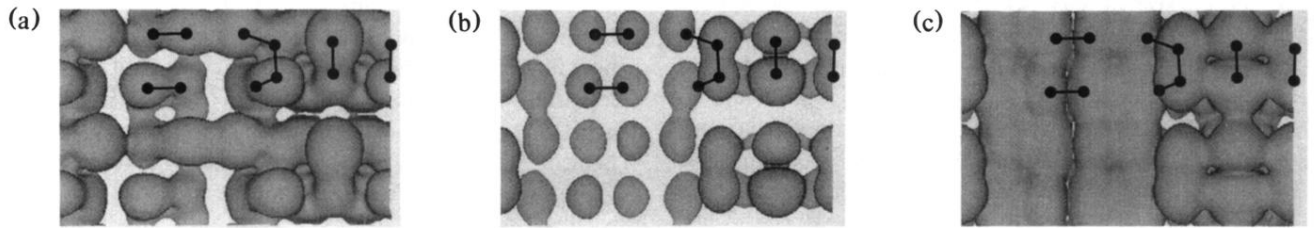


FIG. 2. Simulated STM images of step  $S_B$  with a nonrebonded edge. (a) The filled-state image at a “high-current” condition; (b) the empty-state image at a “high-current” condition; and (c) the filled-state image at a “low-current” condition. The positions of the topmost atoms are denoted by filled circles. See text.